

**Table VIII. Prediction of Hammett  $\sigma$  Values of Substituted Benzoic Acids**

no.	substituent	obs $\sigma$	calculated $\sigma$	
			eq 3	eq 15
1	<i>m</i> -CH=CH <sub>2</sub>	0.05	-0.01	<b>0.02</b>
2	<i>m</i> -CH <sub>2</sub> CN	0.16	0.17	0.14
3	<i>m</i> -CHO	0.35	0.18	<b>0.27</b>
4	<i>m</i> -CH <sub>2</sub> OCH <sub>3</sub>	0.02	-0.03	0.13
5	<i>m</i> -COCH <sub>3</sub>	0.38	0.13	<b>0.26</b>
6	<i>m</i> -CONH <sub>2</sub>	0.28	0.12	<b>0.28</b>
7	<i>m</i> -NCS	0.48	0.34	<b>0.44</b>
8	<i>m</i> -NHCH <sub>3</sub>	-0.30	-0.03	-0.11 <sup>a</sup>
9	<i>m</i> -N(CH <sub>3</sub> ) <sub>2</sub>	-0.15	-0.12	-0.21
10	<i>m</i> -OCOCH <sub>3</sub>	0.39	0.15	0.70
11	<i>m</i> -SCN	0.41	<b>0.35</b>	0.49
12	<i>m</i> -SO <sub>2</sub> NH <sub>2</sub>	0.46	<b>0.64</b>	0.76
13	<i>p</i> -CH=CH <sub>2</sub>	-0.02	-0.04	-0.12
14	<i>p</i> -CH <sub>2</sub> CN	0.01	0.18	<b>0.07</b>
15	<i>p</i> -CHO	0.42	0.34	<b>0.45</b>
16	<i>p</i> -CH <sub>2</sub> OCH <sub>3</sub>	0.03	<b>0.01</b>	-0.15
17	<i>p</i> -COCH <sub>3</sub>	0.50	0.30	<b>0.39</b>
18	<i>p</i> -CONH <sub>2</sub>	0.36	0.30	<b>0.34</b>
19	<i>p</i> -NCS	0.38	0.18	<b>0.19</b>
20	<i>p</i> -NHCH <sub>3</sub>	-0.84	-0.48	-0.49 <sup>b</sup>
21	<i>p</i> -N(CH <sub>3</sub> ) <sub>2</sub>	-0.83	-0.57	-0.58
22	<i>p</i> -SCN	0.52	0.30	<b>0.59</b>
23	<i>p</i> -SO <sub>2</sub> NH <sub>2</sub>	0.57	<b>0.79</b>	0.89 <sup>c</sup>

<sup>a</sup> For a slightly lower energy conformation the calculated  $\sigma$  is -0.28. <sup>b</sup> Equation 14 predicts a  $\sigma$  value of -0.69. <sup>c</sup> Equation 14 predicts a  $\sigma$  value of 0.55. A conformation that is 2 kcal/mol higher in energy has predicted  $\sigma$  values of 0.44 (eq 15) and 0.75 (eq 3).

of a ligand with a macromolecule may involve substituent effects on atoms at more than one position on the ligand. Because in CoMFA one does not measure substituent effects with respect to only one site, but lets the data decide the relationships, CoMFA is more attractive than traditional QSAR to study the electrostatic contributions to substituent effects on bioactivity.

### Methods

**Molecular Modeling.** The starting coordinates were generated with CONCORD.<sup>18</sup> The core benzoic acid conformation was planar. All geometric variables were optimized with AM1 of MOPAC.<sup>19,20</sup> For meta-substi-

(18) Rusinko, A. III; Skell, J. M.; Balducci, R.; McGarity, C. M.; Pearlman, R. S. The University of Texas at Austin and Tripos Associates, St. Louis, MO, 1988.

tuted benzoic acids, the conformation chosen has the substituent on the same side of the molecule as the carbonyl oxygen of the acid. The molecules were aligned by superimposing the unsubstituted benzoic acid moiety.

Partial atomic charges were calculated with AM1 or our modification of the method of Weiner, et al.<sup>17</sup> described above. (For sulfur atoms the MNDO parameters were used in AM1.) The coordinates and partial atomic charges for each molecule are in the supplemental material.

**CoMFA Descriptor Calculation.** The steric and electrostatic CoMFA descriptors were obtained by first calculating the interaction energies with the program GRID. A zero van der Waals radius and a charge of 1.0 was used for the H<sup>+</sup> probe and a radius of 1.95 Å and a charge of 0.0 was used for the methyl probe. For each molecule the energies at a total of 720 grid points were calculated with 2-Å spacing in a lattice of 14 × 16 × 18 Å.

Several considerations reduced the number of points to be considered with PLS. All steric energies with a value greater than 4.0 kcal/mol were truncated to 4.0. Any lattice point for which the standard deviation is less than 0.05 was discarded. To select only electrostatic energies calculated outside the union volume of the molecules in the dataset, we discarded any lattice point for which the steric energy for any molecule of the dataset is 4.0 kcal/mol or greater. For example, these procedures reduced the number of lattice points to 656, 654, and 637 for eqs 13, 14, and 15.

**PLS Calculations.** Because of earlier experience (manuscript in preparation) we did not use the standard PLS method, but instead a modification of it. We first extracted 10 orthogonal latent variables by the standard PLS algorithm. We observed that the order of extraction might not be the order of the correlation of the variables with the dependent property. Therefore, we added the variables to the equation in the order of their correlation with the dependent variable. The "best model" was chosen as that which minimizes the sum of squares of (predicted minus observed) using predictions made from leave-one-out jackknife method.

**Supplementary Material Available:** Coordinates and AM1 partial atomic charges for 49 benzoic acids (49 pages). Ordering information is given on any current masthead page.

(19) Stewart, J. J. P. MOPAC V5.0 (QCPE No. 455). Ran with the keywords NOINTER and XYZ.

(20) Dewar, M. J. S.; Zoebisch, E. G.; Healy, E. F.; Stewart, J. J. P. *J. Am. Chem. Soc.* 1985, 107, 3902.

## The Perimeter Model and Magnetic Circular Dichroism of Porphyrin Analogues

Jacek Waluk<sup>1</sup> and Josef Michl\*

Center for Structure and Reactivity, Department of Chemistry and Biochemistry, The University of Texas at Austin, Austin, Texas 78712-1167

Received July 16, 1990

The simple perimeter model is used to analyze the electronic structure of a series of conjugated macrocycles formally related to the C<sub>20</sub>H<sub>20</sub><sup>2+</sup> perimeter, such as porphyrin, porphycene, secophyrin (parent of texaphyrin), and several that have not yet been synthesized. Particular attention is paid to consequences for UV-vis absorption and magnetic circular dichroism and to the effect of substitution and benzo annelation on these properties.

It has been known for some time that magnetic circular dichroism (MCD) of numerous cyclic approximately or

exactly planar  $\pi$ -electron systems may be not only successfully computed at the semiempirical PPP or INDO/S

level, but also interpreted in terms of the perimeter model.<sup>2,3</sup> The two approaches are complementary in that the computer calculations produce results for a large number of excited states of a molecule (however, only those for the first few tend to be reliable), while the simple model that goes back to Platt<sup>4</sup> only treats the most prominent few states but yields physical insight into the origin of the numerical results and their relation to molecular structure. It is particularly useful for the understanding of trends in a series of related structures and is likely to remain valuable for the simple insight it provides, even long after the present-day semiempirical procedures of computation have yielded to ab initio procedures as computer technology advances.

The attractiveness of the perimeter model description of MCD spectra is primarily due to the fact that after some algebra it yielded formulas that have been derived once and for all and that express the MCD intensities in terms of state energies (taken from experiment) and of relative orbital energy differences that can be estimated from measurements or calculations. Most importantly, the requisite relative orbital energy differences can usually be estimated with sufficient reliability even at the Hückel or PMO<sup>5</sup> levels with computing tools no more complicated than pencil and paper.

The properties of perimeter MO's follow from symmetry, and different kinds of perturbations (bridging, cross-linking, heteroatom replacement, twisting about a bond, etc.) influence orbital energies in a way that may most often be predicted correctly by using first-order or second-order perturbation theory (PMO<sup>5</sup>), i.e., by using expressions such as  $\Delta k_i = \sum_{\mu} c_{i\mu}^2 \Delta \delta_{\mu} + 2 \sum_{\mu, \nu} c_{i\mu} c_{i\nu} \Delta \rho_{\mu\nu}$  for an intramolecular perturbation described by a change of electronegativity (Hückel Coulomb integral)  $\Delta \delta_{\mu}$  of the AO on the  $\mu$ th atom and a change  $\Delta \rho_{\mu\nu}$  of the Hückel resonance integral between AO's  $\mu$  and  $\nu$ . Here,  $\Delta k_i$  is the change in the energy of the  $i$ th MO, with coefficients  $c_{i\mu}$ , and all energies are in units of  $\beta_{CC}$  (Hückel resonance integral between AO's on neighboring carbons). A simple second-order expression describes intermolecular perturbations (union of two subsystems);  $\Delta k_i \approx \sum_j (\sum_{\mu, \nu} c_{i\mu} c_{j\nu} \rho_{\mu\nu})^2 / (k_i - k_j)$  where  $i$  is a particular MO of one subsystem, attached through its AO  $\mu$  to the atom  $\nu$  of the other subsystem. The first sum runs over all MO's of the latter and the double sum runs over all newly established connections  $\mu$ - $\nu$ , whose resonance integrals are  $\rho_{\mu\nu}$  (in units of  $\beta_{CC}$ ). A detailed description for these and more complicated cases is available in standard textbooks.<sup>5</sup>

The combination of the perimeter model for MCD signs and intensities<sup>2</sup> with PMO theory<sup>5</sup> has accounted for the MCD spectral patterns in well over a hundred molecules derived from aromatic perimeters,<sup>2b</sup> and it would now appear reasonable to use it in a predictive mode for new molecules of this class. In this paper, this concept is applied to an example of a structural family that has recently been of considerable interest. It is shown how chemically identical but topologically different perturbations may lead to completely different patterns of frontier orbital energies and, thus, to a different MCD and absorption behavior. We compare three porphyrinoid structures derived from

the  $C_{20}H_{20}^{2+}$  perimeter: (i) porphyrin 1; (ii) its isomer, porphycene<sup>6</sup> 2; and (iii) "secophyrin" 3, the parent species of the expanded porphyrin, texaphyrin 4<sup>7</sup> ("benzosecophyrin"). We also make predictions for other porphyrinoids 5-15 that may be formally derived from the same perimeter, but whose synthesis still remains to be performed.

## Results and Discussion

**The Perimeter Model for Aromatics.** For molecules that can be derived from a  $(4N + 2)$   $\pi$ -electron  $[n]$ annulene perimeter,<sup>2</sup> the perimeter model considers configuration interaction between the four configurations resulting from single-electron excitations from the two highest occupied (HOMO)  $\pi$ -orbitals, whose energies differ by  $\Delta$ HOMO, into the two lowest unoccupied (LUMO)  $\pi$ -orbitals, whose energies differ by  $\Delta$ LUMO. The resulting four electronic states are labeled  $L_1$ ,  $L_2$ ,  $B_1$ , and  $B_2$  in the order of increasing energy (in the special case of uncharged perimeters,  $n = 4N + 2$ , the subscripts a and b, introduced originally by Platt,<sup>4</sup> are also meaningful:  $L_b$ ,  $L_a$ ,  $B_b$ ,  $B_a$ ). For historical reasons, in porphyrins and related compounds the L transitions are labeled "Q" and the B transitions "Soret."

Integrated MCD intensities are usually expressed through the values of the Faraday  $B$  terms (and also  $A$  and  $C$  terms in the case of high-symmetry molecules). Note that a positive (negative)  $B$  term corresponds to a negative (positive) peak in the MCD spectrum. Algebraic solution of the model led to formulas for the Faraday  $B$  terms that contain two contributions: (i) the so-called  $\mu^-$  contributions, essentially structure independent and small for the  $L_1$  and  $L_2$  transitions, and usually large and dominant for the  $B_1$  and  $B_2$  transitions; (ii)  $\mu^+$  contributions, typically larger in magnitude than the former for the  $L_1$  and  $L_2$  transitions, though usually not for the  $B_1$  and  $B_2$  transitions (unless  $\Delta$ HOMO  $\ll$   $\Delta$ LUMO). The  $\mu^+$  contributions are dictated by the orbital energy differences  $\Delta$ HOMO and  $\Delta$ LUMO and are a sensitive function of the molecular structure. In most cases, they determine the MCD sign pattern of the  $L_1$  and  $L_2$  bands, whereas the  $\mu^-$  contributions determine the MCD sign of the  $B_1$  band and the high-energy  $B_2$  band (which is often difficult to identify). According to the algebraic solution, the sign pattern of the  $\mu^+$  contributions corresponds to a +, -, +, - sequence of  $B$  term signs for the  $L_1$ ,  $L_2$ ,  $B_1$ , and  $B_2$  transitions when  $\Delta$ HOMO  $>$   $\Delta$ LUMO and to a -, +, -, + sequence when  $\Delta$ HOMO  $<$   $\Delta$ LUMO.

When  $\Delta$ HOMO =  $\Delta$ LUMO, the  $\mu^+$  contributions vanish and the MCD sign pattern is determined by  $\mu^-$  terms alone. For almost all values of  $n$  and  $N$ , it is +, +, -, +. In this case, even a slight perturbation may destroy the equality of  $\Delta$ HOMO and  $\Delta$ LUMO, inducing a change in the MCD signs. Therefore, molecules for which  $\Delta$ HOMO and  $\Delta$ LUMO are equal have been labeled "soft" MCD chromophores.<sup>2</sup> When the equality is exact, and  $\Delta$ HOMO =  $\Delta$ LUMO  $\neq$  0, one of the L transitions may have vanishing absorption intensity in the model even if it is symmetry allowed. Whether such vanishing intensity is indeed induced by the equality of  $\Delta$ HOMO and  $\Delta$ LUMO depends on the molecular symmetry if the perimeter is uncharged ( $n = 4N + 2$ ), but it is always expected for  $L_2$  if the perimeter is charged. When  $\Delta$ HOMO =  $\Delta$ LUMO = 0, the

(1) Permanent address: Institute of Physical Chemistry, Polish Academy of Sciences, 01-224 Warsaw, Kasprzaka 44, Poland.

(2) (a) Michl, *J. J. Am. Chem. Soc.* 1978, 100, 6801, 6812, 6819. (b) Michl, *J. Tetrahedron* 1984, 40, 3845.

(3) Höweler, U.; Chatterjee, P. S.; Klingensmith, K. A.; Waluk, J.; Michl, *J. Pure Appl. Chem.* 1989, 61, 2117.

(4) Platt, J. R. *J. Chem. Phys.* 1949, 17, 484.

(5) Dewar, M. J. S.; Dougherty, R. C. In *The PMO Theory of Organic Chemistry*; Plenum Press: New York, 1975.

(6) Vogel, E.; Köcher, M.; Schnickler, H.; Lex, J. *Angew. Chem., Int. Ed. Engl.* 1986, 25, 257.

(7) Sessler, J. L.; Murai, T.; Lynch, V.; Cyr, M. *J. Am. Chem. Soc.* 1988, 110, 5586.

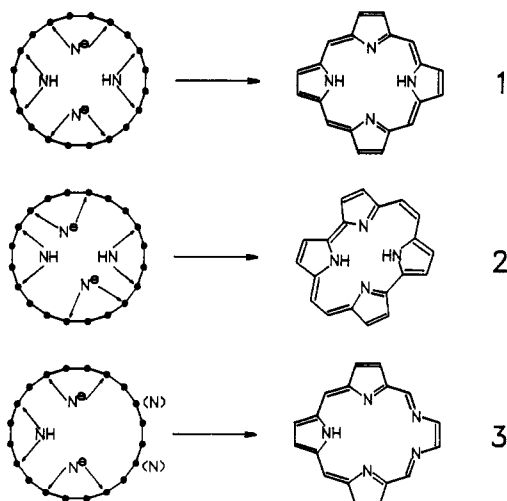


Figure 1. Formal derivation of porphyrin (1), porphycene (2), and secophyrin (3) from a  $C_{20}H_{20}^{2+}$  perimeter.

purely electronic intensities of both L transitions vanish ("double soft chromophores").

The cyclic  $\pi$ -electron structures for which  $\Delta HOMO > \Delta LUMO$  are called "positive-hard" chromophores and the ones with  $\Delta HOMO < \Delta LUMO$  "negative-hard" chromophores,<sup>2</sup> where the first part of the name indicates the sign of the  $B$  term for the  $L_1$  transition, while the second reflects the fact that in this type of a chromophore it is not easy for a substituent, heteroatom, or other weak perturbations to change the MCD sign pattern. In hard chromophores, both L bands have considerable absorption intensity.

The perimeter model generally does very well for the lowest two or three excited states. At higher energies, magnetic mixing with other states, not considered in the model, usually becomes important and invalidates the results. A much more detailed description of the model, including results for polarization directions as well as MCD, is available elsewhere.<sup>2</sup>

**Applications to the Macrocycles 1-3.** Figure 1 shows the formal derivation of porphyrin (1), porphycene (2), and secophyrin (3) from a  $C_{20}H_{20}^{2+}$  perimeter. It is achieved by distorting the shape of the perimeter and introducing the donor  $-NH-$  bridges and the even more strongly donating  $-N-$  bridges. In the case of secophyrin, this is followed by replacing two  $-CH=$  groups by aza nitrogens,  $-N=$ .

The first-order response of a particular perimeter orbital to a perturbation may be predicted upon inspection of its nodal properties, which dictate the values of LCAO coefficients. If a bridging atom is placed in a nodal plane of an orbital, no change of energy should occur since the contributions from the two new bond resonance integrals cancel. One should expect orbital energy changes to increase as the algebraic sum of the LCAO coefficients in the positions of bridging becomes larger and as the bridging atom becomes a better donor ( $-N-$  in place of  $-NH-$ ).

Figure 2 presents the symmetry-adapted HOMO and LUMO orbitals of the parent  $C_{20}H_{20}^{2+}$  perimeter and the predicted orbital energy pattern after the perturbations leading to 1, 2, and 3. The  $s$  and  $a$  labels reflect symmetry and antisymmetry of the unperturbed perimeter orbitals, respectively, with respect to the plane containing both  $-NH-$  bridges and perpendicular to the plane of the perimeter. Totally different patterns arise for each compound.

(i) In porphyrin (1), the LUMO orbitals  $-s$  and  $-a$  should be stabilized to a similar degree (to the same degree in porphyrin dication and dianion, when all four perturbing bridges are identical and the LUMO pair is degenerate by symmetry). The energy of the HOMO orbital  $a$  should not change, since the bridging atoms lie in the nodal plane. The energy of the  $s$  orbital should also remain practically unchanged, since the attachment points lie almost exactly on nodes. To first order, one thus expects similar and nearly vanishing values of  $\Delta HOMO$  and  $\Delta LUMO$ . This means that 1 should be a double soft chromophore and the

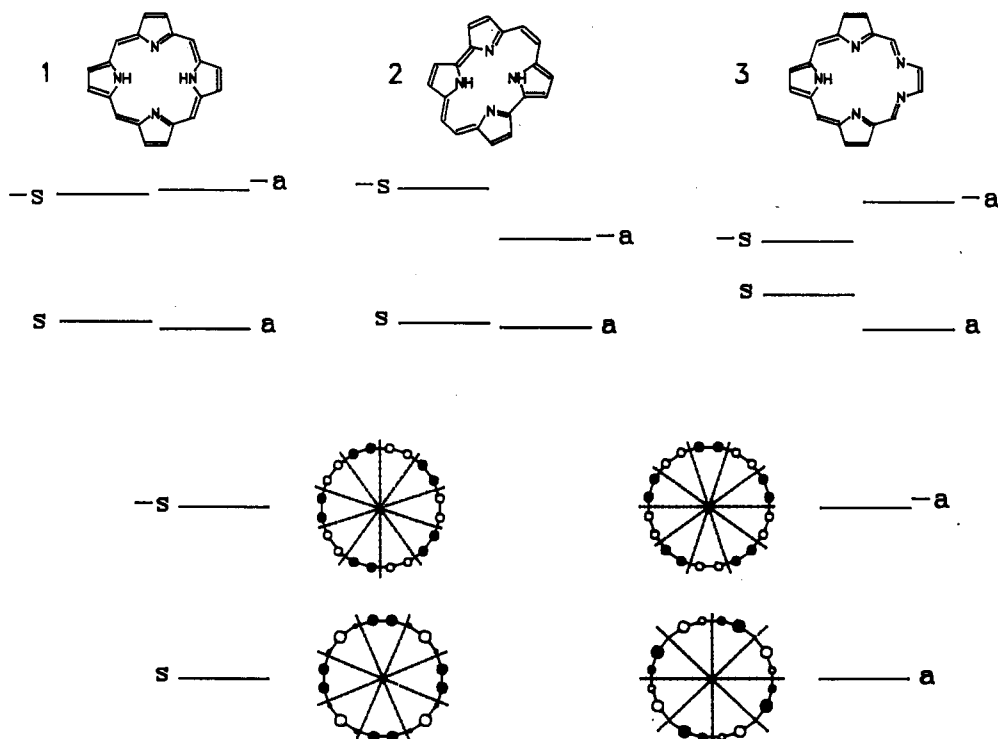


Figure 2. Frontier orbitals of the  $C_{20}H_{20}^{2+}$  perimeter (bottom) and the predicted orbital energy sequences in porphyrin (1), porphycene (2), and secophyrin (3) (top).

Table I. Comparison of Predicted and Calculated Orbital Splittings of Various Porphyrinoids

	bridging positions	PMO	PPP <sup>a</sup>			
			(eV)		(10 <sup>3</sup> cm <sup>-1</sup> )	
			$\Delta$ HOMO	$\Delta$ LUMO	L <sub>1</sub>	L <sub>2</sub>
1 (porphyrin)	1/4, 6/9, 11/14, 16/19	$\Delta$ HOMO $\approx$ $\Delta$ LUMO	0.82	0.07	13.5	16.3
5	1/4, 6/9, 12/15, 17/20	$\Delta$ HOMO $\approx$ $\Delta$ LUMO	0.11	0.05	17.3	19.9
6	1/4, 5/8, 12/15, 16/19	$\Delta$ HOMO $\approx$ $\Delta$ LUMO	0.04	0.30	16.6	19.7
7	1/4, 5/8, 10/13, 15/18	$\Delta$ HOMO $\approx$ $\Delta$ LUMO	0.29	0.69	17.1	18.0
8	1/4, 5/8, 12/15, 17/20	$\Delta$ HOMO < $\Delta$ LUMO	0.20	0.56	17.3	17.7
2 (porphycene)	1/4, 7/10, 11/14, 17/20	$\Delta$ HOMO $\ll$ $\Delta$ LUMO	0.37	1.89	13.0	15.4
9	1/4, 5/8, 11/14, 17/20	$\Delta$ HOMO $\ll$ $\Delta$ LUMO	0.37	1.88	13.1	15.2
10	1/4, 5/8, 9/12, 17/20	$\Delta$ HOMO $\ll$ $\Delta$ LUMO	0.32	1.74	12.9	15.4
11	1/4, 5/8, 9/12, 13/16, 17/20	$\Delta$ HOMO $\ll$ $\Delta$ LUMO	0.44	2.60	14.1	15.4

<sup>a</sup>MMX optimized geometry used in input (PCMODEL, Serena Software, Bloomington, IN).

MCD *B* terms of its L and B transitions should be dominated by further perturbations present. This is indeed observed experimentally.<sup>8-11</sup> In actual fact,  $\Delta$ HOMO turns out to be slightly larger than  $\Delta$ LUMO, but this is not obvious from the first-order approximation. The PPP method with standard parameters tends to exaggerate this difference (Table I), but at the 3-21G ab initio level, it is only 0.24 eV ( $\Delta$ HOMO = 0.33 eV,  $\Delta$ LUMO = 0.09 eV).<sup>12</sup> The near equality of the nearly vanishing  $\Delta$ HOMO and  $\Delta$ LUMO is also reflected in the low intrinsic intensities of both Q bands. The observed intensities are mostly borrowed from the Soret bands by vibronic interactions.

(ii) A different situation occurs in porphycene<sup>13</sup> (2). Now, the two HOMO orbitals should be approximately degenerate, whereas the LUMO orbitals should be arranged so that  $-a$  lies below  $-s$ . The resulting inequality,  $\Delta$ HOMO <  $\Delta$ LUMO, implies a  $-$ ,  $+$ ,  $-$ ,  $+$  sequence of  $\mu^+$  contributions to the *B* terms, characteristic of a negative-hard chromophore, and provides fair intensity for both L transitions. Experimental results<sup>13</sup> are in excellent agreement with these expectations.

(iii) In our third example, secophyrin (3), simple perturbation theory predicts the  $-s$ ,  $-a$  ordering of the LUMO's. The *a* orbital should be stabilized by the double aza replacement to a much larger degree than the *s* orbital. This should lead to the near-equality,  $\Delta$ HOMO  $\approx$   $\Delta$ LUMO  $\neq$  0, and it is not possible to estimate with certainty which of the two quantities is larger. In such a case, the MCD may well be determined by  $\mu^-$  contributions, which give small and positive *B* terms for both L transitions. The absorption intensity of the L<sub>2</sub> transition would then be much weaker than that of L<sub>1</sub>. The *a*, *s*,  $-s$ ,  $-a$  sequence, and the approximate equality of  $\Delta$ HOMO and  $\Delta$ LUMO expected for secophyrin, cannot be checked against experiment, since this molecule has not yet been synthesized.<sup>14</sup>

**Application to the Macrocycles 5–11.** Using this type of approach, we may predict orbital splittings and thus the MCD behavior of various other porphyrinoid structures that may be derived from the C<sub>20</sub>H<sub>20</sub><sup>2+</sup> perimeter (Figure

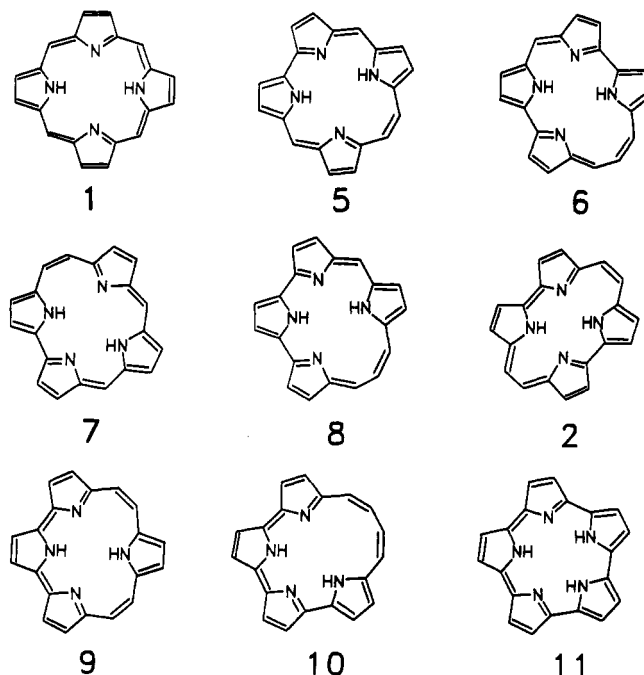


Figure 3. Porphyrinoid structures derived from a C<sub>20</sub>H<sub>20</sub><sup>2+</sup> perimeter, arranged from top left to bottom right in the order of decreasing  $\Delta$ HOMO -  $\Delta$ LUMO values (Table I).

3). Some of these may be expected to prefer quite strongly nonplanar geometries, even in the form of metal complexes, but the predictions of the perimeter model are essentially dictated by the nodal properties of the perimeter orbitals and are quite insensitive to the loss of exact planarity. Since both HOMO orbitals respond very little to bridging (but would be sensitive to aza replacement, as in 3), the resulting MCD pattern is determined primarily by the behavior of the LUMO orbitals. This will be crucially dependent on the position of the bridges. For porphyrin (1) and the structures 5 and 6, two bridges raise the energy of the  $-s$  orbital and two raise the energy of the  $-a$  orbital. This leads to practically no splitting,  $\Delta$ LUMO  $\approx$  0. In the other extreme, in porphycene (2) and the structures 9 and 10, all four bridges will selectively raise the energy of the  $-s$  orbital, while the position of the  $-a$  orbital will not be changed. Thus, a large value of  $\Delta$ LUMO is expected, leading to negative-hard chromophores. The structures 7 and 8 are intermediate between porphyrin-type and porphycene-type chromophores: three of the bridges interact with the  $-s$  orbital, one with the  $-a$  orbital. The inequality  $\Delta$ HOMO <  $\Delta$ LUMO is expected, with  $|\Delta$ HOMO -  $\Delta$ LUMO| smaller than in porphycene. The structure 11 in Figure 3 should provide an example of an extremely hard (negative) MCD chromophore, since all five bridges interact with the  $-s$  orbital only.

(8) Goldbeck, R. A. *Acc. Chem. Res.* 1988, 21, 95.

(9) Goldbeck, R. A.; Tolf, B.-R.; Wee, A. G. H.; Shu, A. Y. L.; Records, R.; Bunnenberg, E.; Djerassi, C. *J. Am. Chem. Soc.* 1986, 108, 6449.

(10) Djerassi, C.; Lu, Y.; Waleh, A.; Shu, A. Y. L.; Goldbeck, R. A.; Kehres, L. A.; Crandell, C. W.; Wee, A. G. H.; Kniezinger, A.; Gaste-Holmes, R.; Lowe, G. H.; Clezy, P. S.; Bunnenberg, E. *J. Am. Chem. Soc.* 1984, 106, 4241.

(11) Keegan, J. D.; Stolzenberg, A. M.; Lu, Y.-C.; Linder, R. E.; Barth, G.; Moscowitz, A.; Bunnenberg, E.; Djerassi, C. *J. Am. Chem. Soc.* 1982, 104, 4305, 4317.

(12) Balaji, V.; Michl, J. Unpublished results.

(13) Waluk, J.; Mueller, M.; Boersch-Pulm, B.; Koecher, M.; Vogel, E.; Hohlneicher, G.; Michl, J. *J. Am. Chem. Soc.*, in press.

(14) A dicyano derivative of this ring system has just been synthesized: Mallouk, T. E.; Hemmi, G.; Sessler, J. L. *Inorg. Chem.* 1990, 29, 3738.

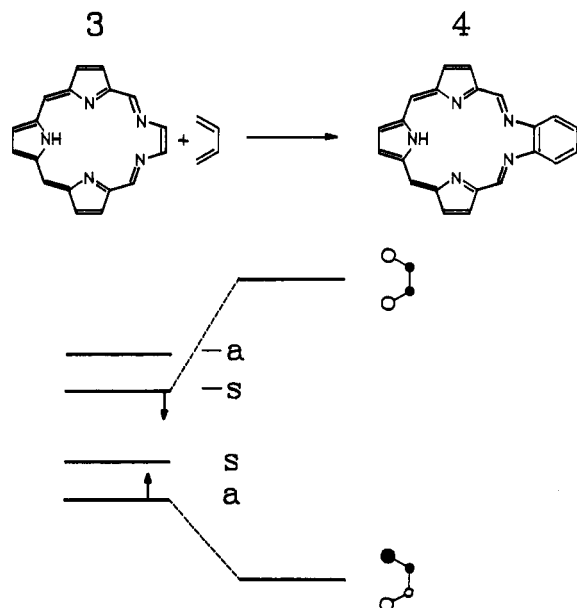


Figure 4. Relation of the frontier orbital energies of texaphyrin (4) and secophyrin (3).

The trends in the relative size of  $\Delta\text{HOMO}$  and  $\Delta\text{LUMO}$  suggested by PMO theory run quite parallel to those obtained by PPP<sup>15</sup> calculations for exactly planar models of all the molecules shown in Figure 3. A comparison is presented in Table I. The only major discrepancy is the already noted tendency of the PPP method to exaggerate the value of  $\Delta\text{HOMO} - \Delta\text{LUMO}$  in porphyrin (1), and we believe the PMO results to be a qualitatively reliable guide to the classification of these macrocycles as soft (1, 5–8) and negative-hard (2, 9–11). Quantitatively accurate predictions of the  $B$  terms probably cannot be presently obtained from any theory, but the signs and values of the  $B$  terms calculated at the PPP-CI level agree qualitatively with the expectations based on the perimeter model and on the relative magnitudes of  $\Delta\text{HOMO}$  and  $\Delta\text{LUMO}$  obtained at the PMO level.

**Application to Texaphyrin 4.** Secophyrin (3) may be regarded a precursor of compounds of the texaphyrin (4) series,<sup>7</sup> whose MCD spectra we have measured recently.<sup>16</sup> The parent texaphyrin (benzannelated secophyrin) may be formally derived from 3 by union with *s-cis*-butadiene (Figure 4). Symmetry dictates that this should destabilize the *a* orbital, which interacts with the HOMO of butadiene, and stabilize the *-s* orbital, which interacts with the LUMO of butadiene. Hence, the *-s*, *-a* sequence of LUMO's, already present in secophyrin (3), is predicted unambiguously to be also present in texaphyrin 4. However, the ordering of the HOMO orbitals will be *s*, *a* if the secophyrin–butadiene interaction is strong enough to reverse the *a*, *s* order predicted for secophyrin. If the interaction is not strong enough, the *a*, *s* sequence will remain, but  $\Delta\text{HOMO}$  in texaphyrin (4) will be reduced with respect to secophyrin (3).

**Substituent Effects.** In this situation, a crucial test for the orbital energy ordering can be provided by the study of substituent effects in MCD spectra. This was used in the past to establish the presence of strong transannular interaction in methano-bridged [10]-annulenes.<sup>17</sup> For a position labeled “dominant” (D), the

effect of a purely conjugative substituent is to increase  $\Delta\text{HOMO}$  ( $-E$ ,  $\pi$ -electron-donating substituents) or to increase  $\Delta\text{LUMO}$  ( $+E$ ,  $\pi$ -electron-accepting substituents). The opposite is true for a “subdominant” (S) position, where the splitting decreases with the increasing strength of the substituent until the substituent effect is so strong that it reverses the initial orbital energy ordering. For a position labeled “neutral” (N), the substituent does not cause significant changes in orbital splittings. The effects of  $\pi$ -donor substituents on the LUMO energies and the effects of  $\pi$ -acceptor substituents on the HOMO energies can be neglected in the first approximation because of the energy mismatch.

A similar classification may also be used for inductive substituents. Now, an overall effect on  $\Delta\text{HOMO} - \Delta\text{LUMO}$  needs to be considered. A dominant position is defined<sup>18</sup> as that for which  $\Delta(\Delta\text{HOMO} - \Delta\text{LUMO})/(-\Delta\alpha)$  is negative (electron-withdrawing  $+I$  substituents decrease and electron-donating  $-I$  substituents increase the value of  $\Delta\text{HOMO} - \Delta\text{LUMO}$ ). A subdominant position is characterized by a positive value of  $\Delta(\Delta\text{HOMO} - \Delta\text{LUMO})/(-\Delta\alpha)$  ( $+I$  substituents increase and  $-I$  substituents decrease the value of  $\Delta\text{HOMO} - \Delta\text{LUMO}$ ). Substitution in a neutral position does not significantly change the difference between HOMO and LUMO splittings. To first order, the value of  $\Delta(\Delta\text{HOMO} - \Delta\text{LUMO})/(-\Delta\alpha)$  may be expressed in terms of LCAO coefficients and equals  $c_2^2 - c_1^2 + c_{-2}^2 - c_{-1}^2$ , where the subscripts 2, 1,  $-1$ ,  $-2$  label the four frontier orbitals in the order of increasing energy.

The assignment of a particular position as D or S refers to the properties of the parent species, as dictated by its orbital energy ordering. If this is reversed by a sufficiently strong perturbation, a dominant position will start to behave as a subdominant one and vice versa. Therefore, experimental evidence that a particular position behaves according to a theoretical prediction (which may be based on calculations, estimations, or just assumptions about energy ordering) provides a strong argument for the orbital sequence determination. In the following paper,<sup>16</sup> we use these principles to show that the observed MCD spectra of various substituted metallohexaalkyltexaphyrins demand the *s*, *a*, *-s*, *-a* orbital sequence assignment for metallotexaphyrin alkylated in all pyrrole ring positions.

Figures 5–7 show the frontier orbitals of porphyrin (1), porphycene (2), and secophyrin (3). Inspection of these orbitals makes it possible to establish a position type with respect to both  $E$  and  $I$  effects and thus permits the use of the perimeter model for the prediction and interpretation of substituent effects on MCD spectra.

The response of porphyrin (Figure 5) to various types of substituents and to inner proton tautomerism, which may lead to a reversal of the signs of MCD  $B$  terms, in terms of the perimeter model, has already been extensively discussed.<sup>8–11</sup>

Porphycene (Figure 6) is a hard chromophore, and its MCD sign pattern is not expected to change easily upon substitution. Still, it may be worthwhile to point out some trends expected for this class of compounds. The positions containing the nitrogen atoms are calculated to be subdominant with respect to inductive substitution. In such a case, one expects  $+I$  substituents to make the value of  $\Delta\text{HOMO} - \Delta\text{LUMO}$  less negative and to decrease the absolute value of the  $B$  terms of the  $L_1$  and  $L_2$  transitions. We have indeed observed such behavior upon passing from

(15) Pariser, R.; Parr, R. G. *J. Chem. Phys.* 1953, 21, 466. Pople, J. A. *Trans. Faraday Soc.* 1953, 49, 1375.

(16) Waluk, J.; Hemmi, G.; Sessler, J. L.; Michl, J., the immediately following paper in this issue.

(17) Klingensmith, K. A.; Püttmann, W.; Vogel, E.; Michl, J. *J. Am. Chem. Soc.* 1983, 105, 3375.

(18) Wallace, S. L.; Michl, J. *Tetrahedron* 1980, 36, 1531.

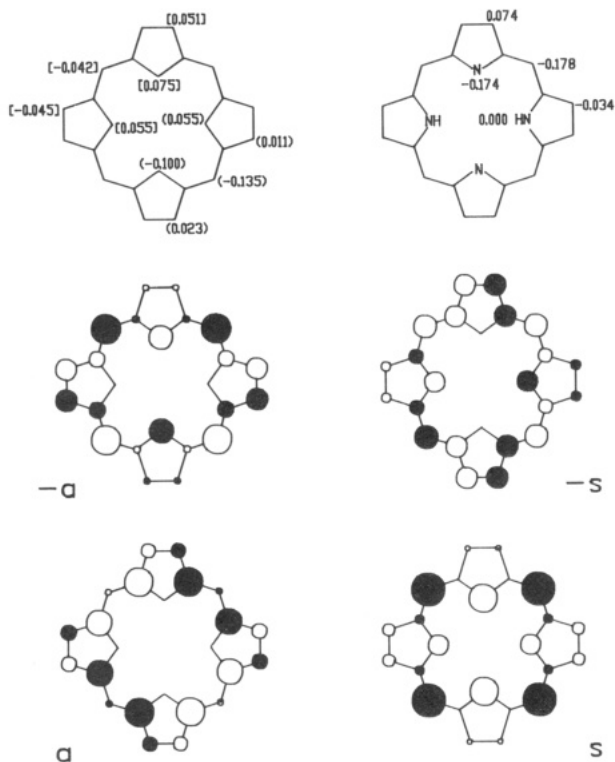


**Figure 5.** Key: bottom, PPP frontier orbitals of porphyrin; top, position type with respect to E (left) and I (right) substituents; left, the difference  $c_2^2 - c_1^2$  (in parentheses) and the difference  $c_{-2}^2 - c_{-1}^2$  (in brackets); right, the difference  $c_2^2 - c_1^2 + c_{-2}^2 - c_{-1}^2$ . See text for details.

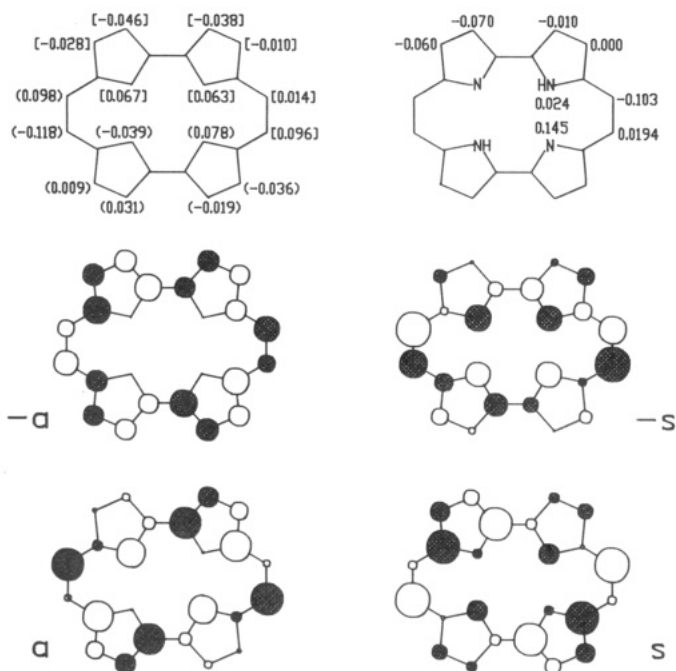


**Figure 6.** Key: bottom, PPP frontier orbitals of porphycene; top, position type with respect to E (left) and I (right) substituents. See caption to Figure 5.

porphycene to porphycene dication and tetraoxaporphycene dication.<sup>13</sup> Inductive substitution at the carbon atoms of the ethylene bridges should cause the opposite response. The positions closer to the NH containing rings are dominant, and those farther from them are subdominant. This difference may be useful for studying tautomeric equilibria in porphycenes. Of the two "trans" forms of a porphycene carrying an inductive sub-

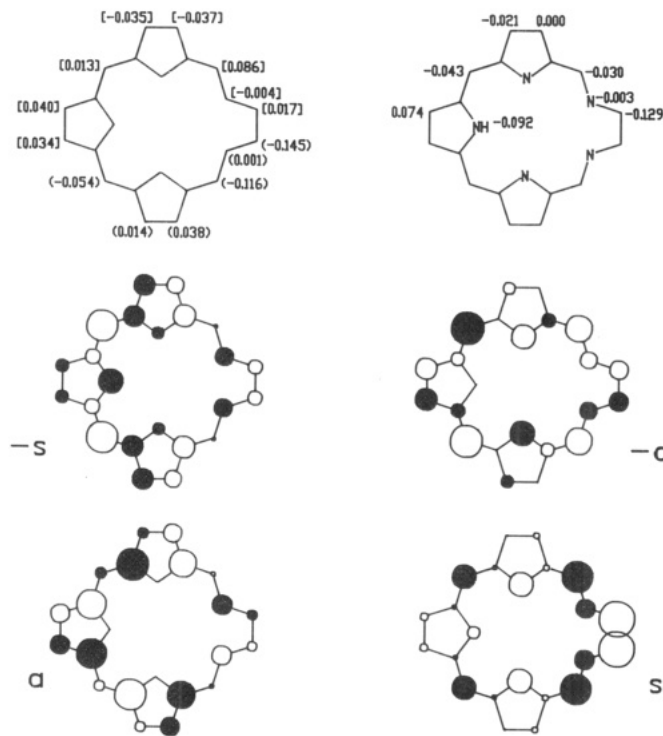


**Figure 7.** Key: bottom, PPP frontier orbitals of secophyrin; top, position type with respect to E (left) and I (right) substituents. See caption to Figure 5.

stituent in this position, with protons on the opposite pyrrole rings, one should have larger  $B$  terms, and the other smaller  $B$  terms, than unsubstituted porphycene. For the "cis" form, with protons on the adjacent pyrrole rings, the effects of the two positions of the ethylene bridges will mutually cancel and  $B$  terms similar to those of the parent porphycene are expected.

**Application to the Macrocycles 12–15.** Since the perimeter model works so well and so simply for porphyrin and its derivatives, as well as porphycenes, we conclude by indicating briefly its possible further use for predicting frontier orbital patterns and the MCD properties for a few other as yet unknown structures derived from  $C_{20}H_{20}^{2+}$  perimeter. For 12 (Figure 8), PMO considerations predict an a, s, -s, -a sequence, with  $\Delta HOMO < \Delta LUMO$  (negative-hard chromophore). Replacement of four CH groups by nitrogen atoms yields a potentially interesting hexadentate ligand, bisecophyrin (13), and exerts a +I inductive effect that will stabilize mostly the a orbital. This leads to the same orbital energy ordering as previously, but now with similar  $\Delta HOMO$  and  $\Delta LUMO$  values, and 13 is likely to be an approximately soft chromophore.<sup>19</sup> Subsequent double benzannelation leading to 14 should destabilize the a orbital and stabilize the -a orbital to comparable degrees, and hence again produce an approximately soft MCD chromophore. The isomeric double benzannelation that leads to the isomer 15 will again destabilize the a orbital, but now the -s orbital will be stabilized. As a result, we may safely expect  $\Delta HOMO < \Delta LUMO$  in 15 (negative-hard chromophore).

The above predictions were checked by PPP calculations for structures 12–15, using the experimental geometry<sup>20</sup> of a pentagonal bipyramidal metallotetrapyrin derivative. The calculated orbital energy sequences indeed were a, s, -s, -a in 12–14 and s, a, -s, -a in 15.  $\Delta HOMO$  and

(19) A nonaromatic precursor to 13 has recently been prepared: Mody, T.; Sessler, J. L. Private communication.

(20) Sessler, J. L.; Murai, T.; Lynch, V. *Inorg. Chem.* 1989, 28, 1333.

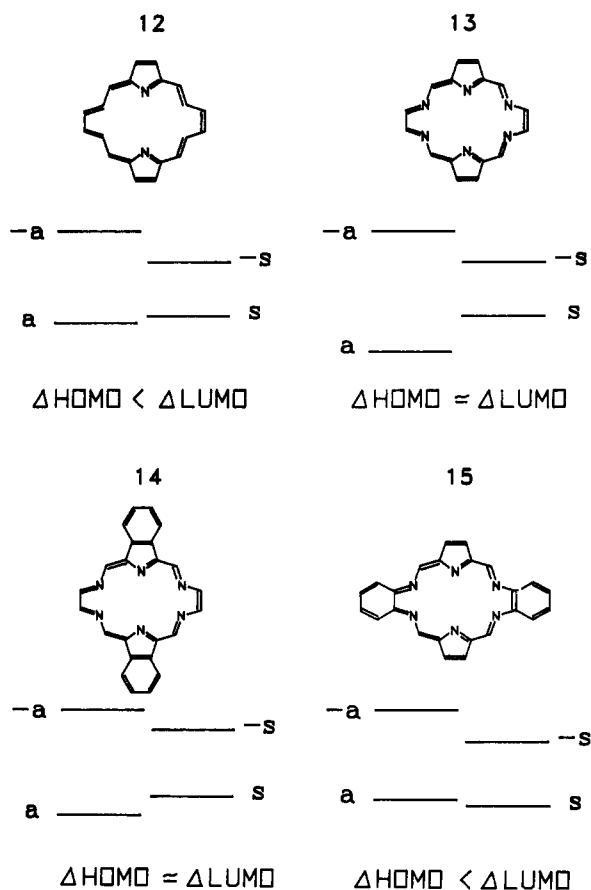


Figure 8. Expected orbital energy patterns for structures derived from a  $C_{20}H_{20}^{2+}$  perimeter.

$\Delta LUMO$  were equal to 0.28 and 0.80 eV in 12, 1.07 and 1.08 eV in 13, 0.14 and 0.73 eV in 14, and 0.12 and 1.92 eV in 15. Except for the orbital splitting in 14, this is in perfect qualitative agreement with PMO expectations. PPP calculations for secophyrin 3 gave the a, s, -s, -a ordering and predicted a soft chromophore character for this compound ( $\Delta HOMO = 0.58$  eV,  $\Delta LUMO = 0.57$  eV).

A numerical computation of the  $B$  term of the  $L_1$  and  $L_2$  bands of 12-15 at the PPP-CI level produced the signs expected from the relative  $\Delta HOMO$  and  $\Delta LUMO$  values.

### Conclusion

The MCD spectra of porphyrins  $1^{8-11}$  and their isomers, the porphycenes 2,<sup>13</sup> have been investigated previously in great detail and have been found to exhibit the qualitative behavior expected from the simple perimeter model.<sup>2a</sup> This makes it likely that the MCD spectra of other related macrocycles will do so as well, similarly as the numerous other cyclic  $\pi$ -electron systems derived from  $(4N + 2)$ -electron perimeters that have been examined in the past.<sup>2b</sup> Indeed, in the following paper<sup>16</sup> the MCD spectra of texaphyrins 4 are shown to be readily interpretable in terms of the perimeter model.

Presently, we have emphasized that the striking difference in the MCD spectral behavior of the nearly double-soft porphyrins and the negative-hard porphycenes readily follows from the difference in their topology by inspection and can be understood without any calculation whatever. We have then proceeded to apply the same principles to a series of the so far unknown related macrocycles 3 and 5-15 and used their topology alone to classify them into a group of soft MCD chromophores 3, 5-8, 13, and 14 and negative-hard chromophores 9-12 and 15, with obvious consequences for their MCD signs and response to perturbation by substituents.

A priori prediction is the true test of a theory. It would not be surprising to find that a numerically complex PPP or INDO/S computer calculation correctly predicts the character of a  $\pi$ -electron MCD chromophore, but it will be a remarkable achievement for a simple procedure based on nothing more than an inspection of molecular structure (topology) to predict correctly a property as complicated as magnetic optical activity, even if it is just for a few low-energy transitions. We leave a verification of the predictions as a challenge to those interested in the preparation and utilization of new macrocyclic ligands.

**Acknowledgment.** This work was supported by the National Science Foundation (CHE 9000292).

## Magnetic Circular Dichroism of Metallotexaphyrins

Jacek Waluk,<sup>1</sup> Gregory Hemmi, Jonathan L. Sessler, and Josef Michl\*

Department of Chemistry and Biochemistry, The University of Texas at Austin, Austin, Texas 78712-1167

Received July 16, 1990

UV-vis absorption and magnetic circular dichroism (MCD) are reported for a series of metal salts of hexaalkyltexaphyrins, recently synthesized novel porphyrinoid structures. The results are interpreted in terms of the standard perimeter model. It is found that texaphyrin is a soft MCD chromophore and that the arrangement of frontier orbitals in metallohexaalkyltexaphyrins is s, a, -s, -a in order of increasing energy.

The derivatives of texaphyrin (1), a recently synthesized<sup>2</sup> "expanded" porphyrin-like system, possess intense near-IR absorption bands and photosensitize the production of singlet oxygen in high yields.<sup>3,4</sup> They are of current in-

terest as possible phototherapeutic agents, and the use of these compounds in magnetic resonance imaging has also been discussed.<sup>5</sup> In addition, texaphyrins are of interest simply as novel ligands, since they are able to support rare coordination geometries such as pentagonal, pentagonal pyramidal, and pentagonal bipyramidal.<sup>6</sup>

Spectral studies of these molecules are in their initial stages. Electronic absorption and fluorescence spectra

(1) Permanent address: Institute of Physical Chemistry, Polish Academy of Sciences, 01-224 Warsaw, Kasprzaka 44, Poland.

(2) Sessler, J. L.; Murai, T.; Lynch, V.; Cyr, M. *J. Am. Chem. Soc.* 1988, 110, 5586.

(3) Maiya, B. G.; Harriman, T.; Sessler, J. L.; Hemmi, G.; Murai, T.; Mallouk, T. E. *J. Phys. Chem.* 1989, 93, 8111.

(4) Harriman, A.; Maiya, B. G.; Murai, T.; Hemmi, G.; Sessler, J. L.; Mallouk, T. E. *J. Chem. Soc., Chem. Commun.* 1989, 314.

(5) Sessler, J. L.; Murai, T.; Hemmi, G. *Inorg. Chem.* 1989, 28, 3390.

(6) Sessler, J. L.; Murai, T.; Lynch, V. *Inorg. Chem.* 1989, 28, 1333.